



Historical simulation of maize water footprints with a new global gridded crop model ACEA

Oleksandr Mialyk¹, Joep F. Schyns¹, Martijn J. Booij¹, Rick J. Hogeboom^{1,2}

¹Multidisciplinary Water Management group, Faculty of Engineering Technology, University of Twente, Enschede, The Netherlands

²Water Footprint Network, Enschede, The Netherlands

Correspondence to: Oleksandr Mialyk (o.mialyk@utwente.nl)

Abstract. Crop water productivity is a key element of water and food security in the world and can be quantified by the water footprint (WF). Previous studies have looked at the spatially explicit distribution of crop WFs but little is known about the temporal dynamics. We develop a new global gridded crop model – AquaCrop-Earth@lternatives (ACEA) – that can simulate three consumptive WF components: green (WF_g), blue from irrigation (WF_{bi}), and blue from capillary rise (WF_{bc}) at high temporal and spatial resolutions. The model is applied to analyse global maize production during 1986-2016 at 5 x 5 arc minute grid. Our results show that in 2012-2016, the global average unit WF of maize is $723.2 \text{ m}^3 \text{ t}^{-1} \text{ y}^{-1}$ (89.5 % WF_g , 8.3 % WF_{bi} , 2.2 % WF_{bc}) with values varying greatly around the world. Regions characterised by high agricultural development generally show a small unit WF and its interannual variation, such as Western Europe and Northern America ($WF < 500 \text{ m}^3 \text{ t}^{-1} \text{ y}^{-1}$, $CV < 15\%$). On the contrary, regions with low agricultural development show opposite outcomes, such as Middle and Eastern Africa ($WF > 2500 \text{ m}^3 \text{ t}^{-1} \text{ y}^{-1}$, $CV > 40\%$). Since 1986, the global unit WF of maize has reduced by 34.6 % mainly due to the historical decrease in yield gaps. However, due to the rapid expansion of rainfed and irrigated cropland, the global WF of maize production has increased by 48.8 % peaking at $762.9 \times 10^9 \text{ m}^3 \text{ y}^{-1}$ in 2016. As many regions still have a high potential in decreasing yield gaps, the unit WF of maize is likely to continue reducing, whereas the WF of maize production is likely to continue growing as humanity's rising appetite can lead to further cropland expansion. The simulation of other crops with ACEA is necessary to assess the pressure of overall crop production on ecosystems and freshwater resources worldwide.

1 Introduction

The ever-increasing demand for crops pushes humanity towards the environmental limits of our planet (Campbell et al., 2017; Jaramillo and Destouni, 2015). In particular, crop production is responsible for around 87 % of total water consumption in the world (Hoekstra and Mekonnen, 2012) which, in many places, already exceeds the sustainable limits posing risks to local water security (Hoekstra et al., 2012b; Schyns et al., 2019) and further deterioration can be expected in the future (Wada and Bierkens, 2014; Greve et al., 2018).



30 One way to minimize the pressure on water resources posed by crop production is to increase crop water productivity, i.e. have “more crop per drop” (Giordano et al., 2006). The volume of water needed to produce a unit of a crop can be measured by the water footprint (WF). The consumptive WF of a crop is calculated as the ratio of crop water use (CWU) to crop yield (Hoekstra, 2011). CWU reflects the amount of accumulated evapotranspiration (ET) over the crop’s growing season and can be attributed to two water types: green – water from rainfall, and blue – water from capillary rise and/or irrigation. ET is
35 usually modelled rather than measured in the field, especially if the focus of studies covers large areas or several alternative crop management practices are assessed (e.g. different irrigation strategies or mulches). Crop yields are commonly measured during the harvest but can be also modelled together with ET to explore feedback loops between crop growth and water availability (Hoekstra, 2011).

Since its introduction in 2002, the WF concept has been widely applied to analyse water use in crop production (Feng et al.,
40 2021; Lovarelli et al., 2016). However, most studies either focus on a small geographical extent (e.g. specific watersheds or administrative units) or consider a short time period. The only few global studies focus on the average year 2000 (Mekonnen and Hoekstra, 2011; Siebert and Döll, 2010; Tuninetti et al., 2015), and thus they lack the analysis of historical trends and interannual variability in crop WFs. Moreover, the methods used to estimate the green and blue WFs in these studies can be improved in various aspects: (i) they apply a crop water requirement approach which does not simulate crop growth and its
45 response to abiotic stresses (e.g. from extreme temperatures or water deficits); (ii) the water balance is simulated without considering capillary rise that can be quite relevant in areas with shallow groundwater (Hoekstra et al., 2012a); (iii) green-blue water separation is performed in post-processing rather than tracing it directly during the modelling, which leads to the lower accuracy of WF estimates (Hoekstra, 2019). Alternatively to these studies, crop WFs can be calculated at high spatial and temporal resolutions with process-based global gridded crop models (GGCMs). These models (such as LPJmL, EPIC, and DSSAT) typically simulate crop growth and water use from the underlying biophysical processes in the atmosphere-plant-soil continuum for each grid cell independently or with couplings between grid cells (Müller et al., 2017). Due to high computational demands, there is a limited body of literature that applies GGCMs, with topics varying from irrigation demand estimation (McNider et al., 2015), climate change impact assessment (Rosenzweig et al., 2014; Ruane et al., 2018), and yield gap analysis (Wang et al., 2021). To our knowledge, global crop WFs have never been studied with GGCMs.

55 In this paper, we present a new GGCM – AquaCrop-Earth@lternatives (ACEA) – with a primary focus on crop water productivity. ACEA is a gridded version of FAO’s standalone process-based and water-driven crop growth model AquaCrop (Steduto et al., 2009). This model is widely applied for crop water productivity studies because it requires a small number of inputs to produce reliable estimates of crop yields as well as CWU under different agro-climatic conditions (Araya et al., 2016; Greaves and Wang, 2016; Karandish and Hoekstra, 2017; Maniruzzaman et al., 2015; Chukalla et al., 2015; Zhuo et al., 2016). In recent years, several studies applied originally site-based AquaCrop at the regional scale by coupling it with a
60 GIS software (Lorite et al., 2013; Huang et al., 2019; Han et al., 2020). However, in this implementation, AquaCrop demands inputs for each simulation site as separate files, which increases modelling complexity and makes global crop simulations extremely demanding on computational resources. To overcome this limitation in ACEA, we utilise the open-



65 source version of AquaCrop developed by Foster et al. (2017) – AquaCrop-OS. We optimise AquaCrop-OS for
computationally efficient large scale simulations by minimising the number of input and output files and by parallelising the
modelling procedure. Furthermore, we implement the daily tracing of green and blue water fluxes in each grid cell to allow
accurate estimation of green and blue crop water productivity.

To demonstrate its performance, we apply ACEA to simulate maize WFs during 1986-2016 at 5 x 5 arc minute resolution
(~8.3 km x 8.3 km), while accounting for historical changes in cropland extent. We focus on maize because it is the most-
70 produced crop in the world (FAOSTAT, 2021) and its WFs are not as extensively researched as WFs of other major crops,
such as rice and wheat (Chapagain and Hoekstra, 2011; Mekonnen and Hoekstra, 2010). In our analysis, we reveal temporal
and spatial patterns in both unit WFs of maize (in $\text{m}^3 \text{t}^{-1} \text{y}^{-1}$) and total WFs of maize production (in $\text{m}^3 \text{y}^{-1}$) at global and
regional levels. In the end, we compare our results to estimates from previous studies and discuss both limitations and
advantages of crop water productivity analysis with ACEA.

75 2 Data and methods

2.1 Global gridded crop model ACEA

2.1.1 General model description

The AquaCrop-Earth@lternatives (ACEA) model is a process-based global gridded crop model (GGCM) specifically
developed to calculate crop water productivity at high spatial and temporal resolutions while requiring a minimum set of
80 input data. Each grid cell is simulated independently via a three-stage procedure as shown in Fig. 1.

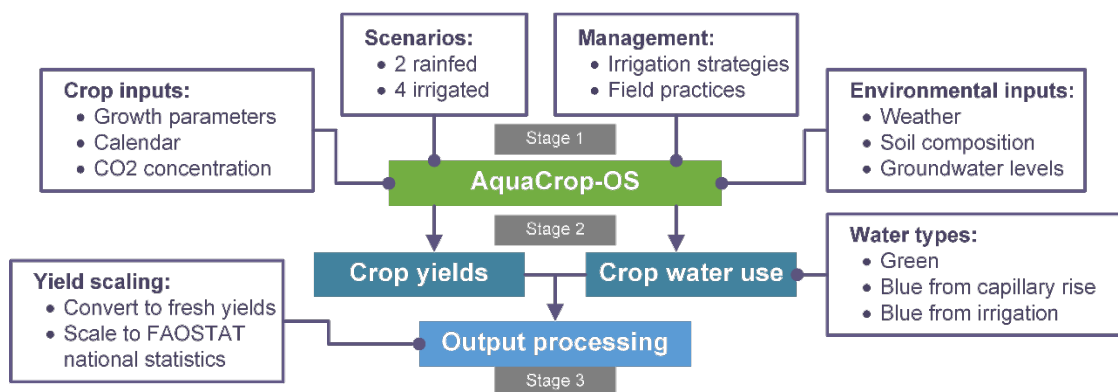


Figure 1: Schematic representation of ACEA's simulation procedure in each grid cell.

In the first stage, ACEA collects crop and environmental input data for each grid cell within the study area. The resolution of
input data determines the size of grid cells, and the geographical extent of rainfed and irrigated crop production systems
85 determines the number of grid cells. Depending on the production system, one or multiple simulation scenarios are selected.
The rainfed scenarios include rainfed (scenario 1) and rainfed with a presence of shallow groundwater (scenario 2). The



irrigation scenarios include surface irrigation (scenario 3), sprinkler irrigation (scenario 4), drip irrigation (scenario 5), and surface irrigation with a presence of shallow groundwater (scenario 6). Besides the simulation scenarios, field management practices (mulches, weed control, and bunds) and customized irrigation strategies are chosen if appropriate. A detailed simulation setup for this study is provided in Sect. 2.1.4.

In the second stage, ACEA runs the AquaCrop-OS crop model (see Sect. 2.1.2) by iterating the grid cells within the study area. AquaCrop-OS simulates the crop growth and soil water balance on a daily time step without considering lateral flows to other grid cells. Thus, the grid cells are independent from each other and can be run in parallel depending on the available computational resources. Main output variables are crop yield and CWU that is attributed to one of the three water types: green, blue from irrigation, and blue from capillary rise. More information about the output variables is provided in Sect. S1.1.

In the third stage, ACEA aggregates the raw outputs from each grid cell into gridded datasets. Then, it runs optional post-processing procedures, such as WF calculation (see Sect. 2.1.3), crop yield scaling (see Sect. 2.1.4), and statistical analyses (see Sect. 2.1.5). The final gridded datasets are saved in a NetCDF format, which allows further crop water productivity analysis in any programming language or GIS software.

2.1.2 AquaCrop-OS

We use AquaCrop-OS version 6.0 (Foster et al., 2017) which is an open-source implementation of FAO's standalone AquaCrop application (Vanuytrecht et al., 2014; Steduto et al., 2009). This crop model is process-based and uses crop, soil, climate, field and irrigation management data to simulate daily crop growth and the soil water balance. The soil water balance is calculated as the sum of water inflow (rainfall, irrigation, and capillary rise) and outflow fluxes (runoff, evapotranspiration, and deep percolation) among soil compartments. Crop development is temperature-driven via growing degree days (GDDs) and is ultimately expressed in biomass build-up. At the end of the growing season, the accumulated biomass is converted into a simulated crop yield via the harvest index, which is affected by water and temperature stresses. Note that AquaCrop-OS v6.0 cannot simulate the nutrient cycle or water salinity. For more information about AquaCrop, please refer to the associated literature (Raes et al., 2009; Steduto et al., 2009; Hsiao et al., 2009).

We have implemented several changes to the original code (see Sect. S1.2). The most important change is the direct separation between green and blue water fluxes based on the method suggested by Hoekstra (2019). On a daily time step, all inflow and outflow water fluxes are accounted separately for every soil compartment. Each of these fluxes is attributed to one of three water types: green, blue from irrigation, and blue from capillary rise. Thus, it is possible to know the composition of soil moisture in terms of these three types when soil evaporation and root water abstraction (equal to crop's transpiration) are calculated. The composition of consumed water is proportional to the water types stored in each soil compartment on a specific time step.



2.1.3 Water footprint calculation

120 ACEA calculates the annual consumptive unit WF ($\text{m}^3 \text{ t}^{-1} \text{ y}^{-1}$) of a crop as the sum of three WF components (Hoekstra, 2011):

$$WF = WF_g + WF_{bc} + WF_{bi} \quad (1)$$

where WF_g is the green WF, WF_{bc} is the blue WF from capillary rise, and WF_{bi} is the blue WF from irrigation. Each WF component is calculated as the ratio of crop water use CWU_x (mm y^{-1}) of a water type x (g , bc , or bi) to crop yield Y ($\text{t ha}^{-1} \text{ y}^{-1}$). To convert from mm y^{-1} into $\text{m}^3 \text{ ha}^{-1} \text{ y}^{-1}$, CWU_x is multiplied by 10:

$$WF_x = \frac{CWU_x * 10}{Y} \quad (2)$$

To obtain Y , the simulated crop yield Y_s in AquaCrop-OS is corrected by two coefficients. The first one is a conversion coefficient from dry to fresh crop yield K_f (0.87 for maize); the second one is a yield scaling factor S , which is introduced to account for external developments not modelled by ACEA (explained in Sect. 2.1.4):

$$130 \quad Y = \frac{Y_s * S}{K_f} \quad (3)$$

The simulated rainfed and irrigated scenarios are combined to analyse rainfed and irrigated production systems. In the case of rainfed systems, the WFs of a water type x from scenario 1 ($s1$) and 2 ($s2$) are simply summed up as rainfed grid cells always have only one of those two scenarios. On the other hand, in irrigated systems, the same grid cell can have several irrigated scenarios at once ($s3$ to $s6$). Therefore, the WF of a water type x from each of the scenarios is multiplied by irrigation factor K_i . The latter is the fraction of irrigated harvested area under the respective irrigation method obtained from Jägermeyr et al. (2015):

$$\left\{ \begin{array}{l} \text{Rainfed } WF_x = WF_{x,s1} + WF_{x,s2} \\ \text{Irrigated } WF_x = \sum_{i=s3}^{s6} WF_{x,i} * K_i \end{array} \right. \quad (4)$$

2.1.4 Crop yield scaling

Crop yield is scaled to incorporate external developments that cannot be modelled in ACEA. Some developments affect long-term trends in crop yields, such as changes in agricultural inputs (e.g. fertilizers, better crop varieties, machinery) or in environmental conditions (e.g. irrigation water quality). Some developments are short-term and cause interannual variability, such as disruptions due to political (e.g. civil wars), economic (e.g. food prices), and natural reasons (e.g. locust plague, flooding). Since these developments are not modelled in ACEA, Y_s represents the maximum attainable values under water and temperature stresses only. Therefore, following previous studies (Mekonnen and Hoekstra, 2011; Siebert and Döll, 2010), we use yield scaling factors to scale Y_s to the official annual statistics reported by FAO (FAOSTAT, 2021). Because FAO reports crop production at the national scale, these factors are the same for all grid cells within one country regardless of the production system (see Fig. 2).

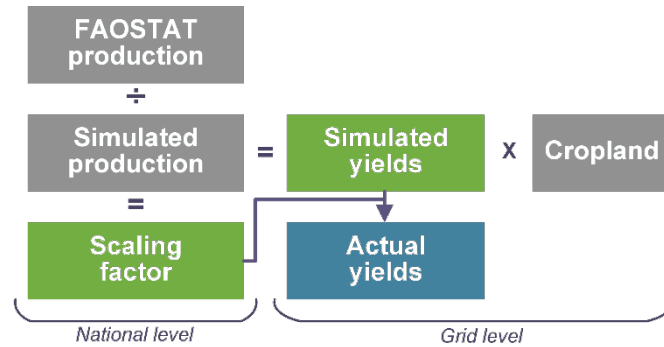


Figure 2: Calculation procedure of yield scaling factor at the national level.

150 The yield scaling factors S are calculated per country per year as the ratio of the official crop production P_{FAO} ($t\ y^{-1}$) reported by FAO to the simulated crop production P_{ACEA} in ACEA. The latter is calculated as the sum of rainfed and irrigated production:

$$S = \frac{P_{FAO}}{\sum Rainfed P_{ACEA} + \sum Irrigated P_{ACEA}} \quad (5)$$

$$\begin{cases} Rainfed P_{ACEA} = \frac{(Y_{s,s1} + Y_{s,s2}) * A_{rainfed}}{K_f} \\ Irrigated P_{ACEA} = \left(\sum_{i=s3}^{s6} \frac{Y_{s,i} * K_i}{K_f} \right) * A_{irrigated} \end{cases} \quad (6)$$

155 where Y_s is the simulated crop yield ($t\ ha^{-1}\ y^{-1}$) in a specific scenario (rainfed: s1 and s2, irrigated: s3 - s6), $A_{rainfed}$ and $A_{irrigated}$ are historical rainfed and irrigated harvested areas ($ha\ y^{-1}$), K_i is the fraction of irrigated harvested area covered by the respective irrigation method in each scenario, and K_f is the conversion coefficient from dry to fresh crop yield.

To account for the historical changes in harvested areas, we extrapolate the MIRCA2000 data to the period of 1986-2016. The extrapolation is performed using two historical datasets on cropland extent HYDE 3.2 and HID (see Table 1) under the
 160 assumption that maize harvested areas experienced the same dynamics as the croplands did. A detailed description of the extrapolation procedure is provided in Sect. S1.7.

The interannual variability in S can lead to large interannual variability in crop yields, and hence in WFs. However, we aim to capture the effect of long-term external conditions while maintaining the modelled climate-related interannual variability. Therefore, we take a three year moving average of scaling factors for each country (using the previous, current, and next
 165 year's factors). This allows to keep the overall trend in historical crop yields and attenuate extreme responses to short-term external developments.



2.1.5 Statistical analyses of results

The statistical analyses in our study are performed at several spatial scales according to the UN classification (UNSD, 2021): global, (sub)regional, and national. To obtain representative values for each scale, the WFs are averaged based on the production amounts, and related WF variables (Y , CWU , and S) are averaged based on the harvested areas in each grid cell. For the trend analysis of WFs and related variables, we use the Mann–Kendall test (Hussain and Mahmud, 2019), which identifies the direction and significance of a trend in time series. We further detrend the variables with significant trends to analyse interannual variations by removing a linear trend. The interannual variability is measured by estimating the coefficient of variation (CV) of detrended timeseries and the dependency between different variables is determined by the Pearson linear correlation coefficient (Brown, 1998).

2.2 Simulation setup

Data needed to run ACEA for global maize production during 1986–2016 are summarised in Table 1. We run ACEA at 30 x 30 arc minute resolution (~50 km x 50 km), which is a common resolution in many GCMs (Franke et al., 2020). The grid cells are selected according to the location of maize production systems obtained from MIRCA2000 (Portmann et al., 2010). We consider one growing season per year and simulation scenarios $s1$ to $s4$ (see Sect. 2.1.1) as $s5$ and $s6$ are not common in maize production.

Table 1: Summary of input data used for maize crop modelling and post-processing in ACEA.

Type	Period	Timestep	Resolution	Source
Data for crop modelling in AquaCrop-OS (1984-2016)				
Climate inputs	1984-2016	daily	30 x 30 arc minutes	GSWP3-W5E5 composite product (Lange, 2019)
Atmospheric CO ₂ concentration	1984-2016	annual	Global average	NOAA (Dlugokencky and Tans, 2020)
Crop parameters	-	-	-	AquaCrop's manual and crop files
Crop calendar	-	-	30 x 30 arc minutes	ISIMIP3 project (ISIMIP, 2020)
Soil composition	-	-	30 x 30 arc minutes	ISIMIP3 project (ISIMIP, 2020) based on Harmonized World Soil Database 1.12 (Nachtergaele et al., 2008)
Groundwater levels	Average of 2004-2014	monthly	5 x 5 arc minutes	Fan et al. (2013)
Data for setup and post-processing (1986-2016)				
Harvested areas	Around 2000	annual	5 x 5 arc minutes	MIRCA 2000 (Portmann et al., 2010)
Irrigated cropland	1985-2005	5 year	5 x 5 arc minutes	HID (Siebert et al., 2015)
Irrigated and rainfed cropland	1980-2017	10 year till 2000 then annual	5 x 5 arc minutes	HYDE 3.2 (Klein Goldewijk et al., 2017)
Maize production statistics	1986-2016	annual	National	FAO (FAOSTAT, 2020)

Climate inputs for AquaCrop-OS are obtained from the GSWP3-W5E5 composite product (Lange, 2019) which provides historical daily rainfall, temperature, surface shortwave radiation, wind speed, and relative humidity. These variables (except



rainfall) are used together with a global elevation model (Amante, 2009) to estimate the potential evapotranspiration according to the Penman-Monteith equation (Allen et al., 1998).

Crop parameters are obtained from the AquaCrop manual (Raes et al., 2018) and default maize crop file provided with AquaCrop-OS. In case of inconsistencies among these two sources, priority is given to data from the manual. The resulting

190 set of maize parameters is generic, and thus crop development stages (in GDDs) for every grid cell are recalculated to ensure that the average growing season duration is similar to the one from the crop calendar (ISIMIP, 2020). This calendar is a composite of multiple recent data sources that rely on national and subnational statistics, remote sensing products, and modelling. Additional information on crop parametrisation is provided in Sect. S1.3.

The soil profile is defined as one layer of 3 m depth with eight compartments ranging from 0.1 to 0.7 m in thickness. The

195 selection of soil compartments is based on the analysis described in Sect. S1.4. Sand, silt, and clay fractions for each grid cell are obtained from the ISIMIP3 project (ISIMIP, 2020) which provides the fractions from the Harmonized World Soil Database 1.12 (Nachtergaele et al., 2008) upscaled to 30 x 30 arc minutes. The soil composition is then converted into hydraulic parameters using a pedotransfer function (Saxton and Rawls, 2006) provided in AquaCrop-OS. To ensure realistic initial soil moisture values, we run the model two years in advance of our study period (as described in Sect. S1.5).

200 The average monthly groundwater levels are taken from Fan et al. (2013) and initially upscaled to 5 x 5 arc minutes using a resample function in QGIS (QGIS, 2021). We further upscale them to 30 x 30 arc minutes by taking average monthly values over underlying 5 x 5 arc minute grid cells where maize production and shallow groundwater (0-3 m in depth) are present. The final groundwater levels are lowered to 1 m depth under the assumption that farmers drain the agricultural field to avoid aeration stress (see Sect. S1.6).

205 Following previous studies (Andarzian et al., 2011; Khoshravesh et al., 2013), irrigation events are triggered as soon as the soil moisture drops below 50 % of the maximum available soil water within the root zone. The amount of irrigated water in each of the irrigated scenarios is limited to field capacity and depends on the percentage of wetted area by the respective irrigation method (Chukalla et al., 2015). The conveyance efficiency is set to 100 % to provide the net irrigation requirement. No particular field management practices are activated due to a lack of data on where they are applied.

210 The simulation results are downscaled to 5 x 5 arc minutes according to the location of rainfed and irrigated maize production systems in MIRCA2000 and location of shallow groundwater levels (only for *sc2*) of the same resolution.

3 Results

3.1 Average maize water footprints in 2012-2016

The global average unit WF of maize is $723.2 \text{ m}^3 \text{ t}^{-1} \text{ y}^{-1}$ in 2012-2016. The share of green water (WF_g) is 89.5 %, while the

215 shares of blue water from capillary rise (WF_{bc}) and irrigation (WF_{bi}) are 2.2 % and 8.3 %, respectively. The distribution of WF around the world is shown in Fig. 3. The map indicates a distinct latitudinal distribution, which corresponds to a similar one in maize yields (see Fig. S1). Small WF values north of 20°N are mainly due to the high yields in main producing



regions: Northern America (WF is $481.2 \text{ m}^3 \text{ t}^{-1} \text{ y}^{-1}$; yield is 10.1 t ha^{-1}), Europe ($581.5 \text{ m}^3 \text{ t}^{-1} \text{ y}^{-1}$; 6.2 t ha^{-1}), and Eastern Asia ($624.6 \text{ m}^3 \text{ t}^{-1} \text{ y}^{-1}$; 5.9 t ha^{-1}). On the other hand, the regions with low maize yields have substantially larger WF values and are mostly located in arid parts of the world that mainly rely on rainfed production systems (e.g. Middle and Eastern Africa). Rainfed systems ($741.9 \text{ m}^3 \text{ t}^{-1} \text{ y}^{-1}$) show a 10 % larger unit WF than irrigated systems ($674.1 \text{ m}^3 \text{ t}^{-1} \text{ y}^{-1}$). However, both the smallest and the largest regional WF (among regions with at least 0.5 % of global maize production) are located in areas dominated by rainfed production (see Table 2), with the largest one in Middle Africa ($3379 \text{ m}^3 \text{ t}^{-1} \text{ y}^{-1}$) and the smallest one in Western Europe ($416.2 \text{ m}^3 \text{ t}^{-1} \text{ y}^{-1}$). The smaller WF in the latter region can be explained by both a smaller CWU (i.e. lower ET rates) and a higher crop yield (see Fig. S1). The WF values also vary among areas dominated by irrigated production. For example, Eastern Asia ($624.6 \text{ m}^3 \text{ t}^{-1} \text{ y}^{-1}$) has a twice smaller WF than Northern Africa ($1170 \text{ m}^3 \text{ t}^{-1} \text{ y}^{-1}$) due to a smaller CWU while the yields in both regions are similar. The global maps with separated rainfed and irrigated maize WF can be found in Fig. S2.

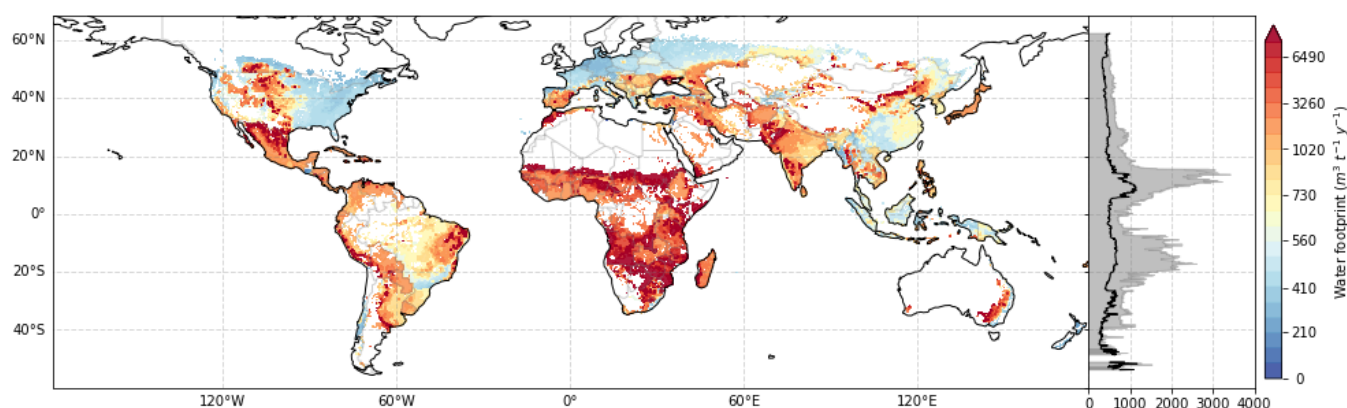


Figure 3: Average unit water footprint of maize in $\text{m}^3 \text{ t}^{-1} \text{ y}^{-1}$ as the average over 2012-2016 at 5 x 5 arc minute resolution. The grey area in the side chart represents the median of all data points along the respective latitude and the black line is the 10 % percentile of them.

Table 2: Overview of global maize production and water footprint statistics as the average over 2012-2016 (except the coefficient of variation (CV) which is estimated for 1986-2016). CWU is crop water use and WF is water footprint (g - green, bc - blue from capillary rise, bi - blue from irrigation). The selection of regions is based on the UN classification (UNSD, 2021).

Region	Maize production [% of global]	Irrigated [% of production]	WF of production [% of global]	Crop yield ($\text{t ha}^{-1} \text{ y}^{-1}$)	Yield gap*	CWU (mm y^{-1})	WF			Unit WF ($\text{m}^3 \text{ t}^{-1} \text{ y}^{-1}$)	Change in unit WF (relative to 1986-1990)	CV of unit WF
							WF_g	WF_{bc}	WF_{bi}			
							(% of unit WF)					
Eastern Africa	3.0%	3.7%	11.3%	1.8	88.1%	505.8	98.3%	0.2%	1.5%	2746.4	-24.3%	55.4%
Middle Africa	0.6%	1.0%	2.9%	1.1	90.6%	375.0	99.2%	0.4%	0.3%	3378.9	-34.9%	41.8%
Northern Africa	0.8%	98.6%	1.3%	5.8	64.2%	674.7	15.1%	0.0%	84.9%	1170.1	-29.4%	8.1%
Southern Africa	1.2%	20.0%	1.6%	4.2	35.4%	429.7	95.7%	0.0%	4.3%	949.3	-65.2%	83.5%
Western Africa	1.9%	0.7%	5.4%	1.6	85.2%	335.8	99.5%	0.3%	0.2%	2066.4	-22.8%	46.4%
Africa	7.4%	15.2%	22.5%	2.0	84.5%	435.5	93.7%	0.3%	6.1%	2169.7	-28.1%	51.3%
Caribbean	0.1%	56.6%	0.2%	1.3	86.4%	299.7	95.3%	0.1%	4.6%	2233.5	-25.3%	25.7%
Central America	2.7%	26.4%	4.5%	3.3	74.7%	364.7	91.4%	0.4%	8.2%	1179.1	-42.7%	16.1%
Northern America	35.3%	18.4%	23.1%	10.1	30.5%	478.1	86.8%	4.0%	9.3%	481.2	-28.6%	13.9%
South America	11.9%	4.7%	12.2%	5.2	63.4%	386.4	96.6%	2.2%	1.2%	741.5	-57.2%	20.5%
Americas	50.0%	15.6%	40.0%	7.4	47.4%	430.6	90.3%	3.0%	6.7%	583.8	-37.1%	15.6%
Central Asia	0.2%	100.0%	0.2%	6.1	46.7%	478.3	31.9%	0.0%	68.1%	778.9	-43.2%	22.4%



Eastern Asia	23.1%	61.0%	19.9%	5.9	55.7%	367.4	82.3%	2.7%	15.0%	624.6	-28.6%	14.4%
South-eastern Asia	4.0%	10.4%	3.6%	4.3	59.5%	277.6	98.2%	0.9%	0.9%	653.9	-59.9%	24.1%
Southern Asia	3.4%	38.3%	4.3%	2.9	71.8%	265.4	87.4%	0.4%	12.2%	906.9	-52.6%	26.4%
Western Asia	0.7%	38.9%	0.5%	7.0	31.6%	394.2	63.1%	0.4%	36.5%	562.4	-41.1%	33.8%
Asia	31.4%	51.7%	28.6%	5.1	58.4%	335.1	84.4%	2.1%	13.6%	658.6	-39.1%	17.4%
Eastern Europe	6.5%	5.2%	5.8%	5.3	52.7%	342.2	94.4%	4.0%	1.5%	655.0	-28.0%	53.6%
Northern Europe	0.015%	12.0%	0.1%	6.4	37.5%	255.0	95.6%	3.5%	1.0%	401.7	-50.2%	56.2%
Southern Europe	2.4%	51.8%	1.8%	7.9	41.3%	427.5	79.5%	5.1%	15.4%	543.2	-28.2%	17.7%
Western Europe	2.2%	21.4%	1.3%	9.1	32.3%	379.4	95.6%	1.3%	3.0%	416.2	-19.7%	9.5%
Europe	11.1%	18.5%	8.9%	6.2	47.2%	361.0	91.6%	3.9%	4.5%	581.5	-24.2%	37.1%
Australia & New Zealand	0.1%	95.4%	0.04%	8.2	30.8%	399.5	66.8%	0.0%	33.1%	490.9	-41.7%	10.5%
Melanesia	0.001%	0.0%	0.001%	5.1	66.1%	320.7	99.2%	0.8%	0.0%	636.6	-72.0%	15.6%
Oceania	0.1%	93.5%	0.04%	8.1	32.1%	397.0	67.6%	0.1%	32.3%	493.7	-42.3%	10.6%
Average world	-	27.3%	-	5.4	58.3%	392.7	89.5%	2.2%	8.3%	723.2	-34.6%	21.3%

235 * yield gap is estimated as: 100 % - yield scaling factor.

Zooming to the national level, the average unit WF of maize of the nine biggest producing nations plus the EU 27 is 592.3 $m^3 t^{-1} y^{-1}$ (88.3 % WF_g , 2.9 % WF_{bc} , and 8.9 % WF_{bi}). Together, they produce 84.3 % of maize globally. The WF values range from 485.3 $m^3 t^{-1} y^{-1}$ in the USA to 1244 $m^3 t^{-1} y^{-1}$ in Mexico (see Fig. 4). The contribution of blue water from capillary rise WF_{bc} is substantial in Argentina (7.6 % of WF), the USA (3.9 %), and the EU 27 (3.4 %). Among the EU 27 countries, the largest WF_{bc} shares are in the Netherlands (26.1 %), Slovakia (13.7 %), and Hungary (9.6 %). The complete table with maize WF s of 148 countries can be found in Table S2.

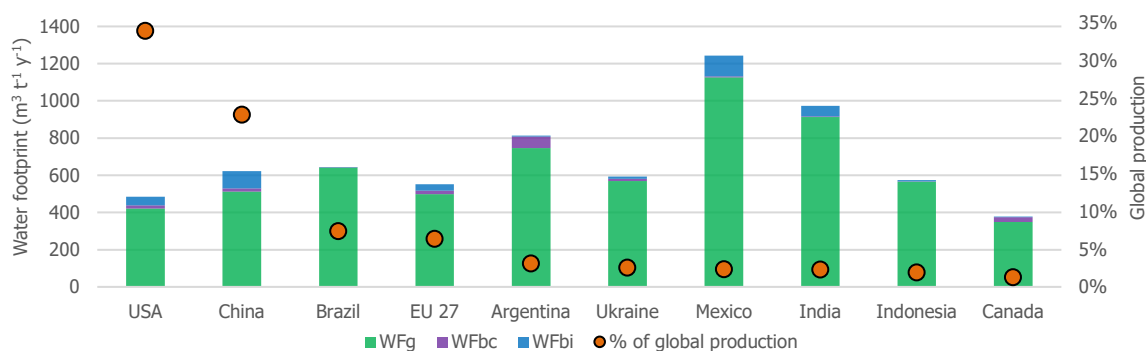


Figure 4: Average unit water footprint (g - green, bc - blue from capillary rise, bi - blue from irrigation) in $m^3 t^{-1} y^{-1}$ and percentage of global production of maize in the ten biggest maize producers during 2012-2016.

245 In terms of the global WF of maize production (i.e. total water consumption), more than 91 % of water is consumed in Americas (40.0%), Asia (28.6%), and Africa (22.5%) as shown in Table 2. The shares of global production in Americas (50.0%) and Asia (31.4%) are larger than the shares of global WF , which indicates high crop water productivities. On the contrary, Africa's share of global production is three times smaller than its share of the global WF , which indicates a low crop water productivity.

250



3.2 Historical trends in maize water footprints

The global average unit WF of maize has reduced over the last decades as shown in Fig. 5. When compared to 1986-1990, the average WF of 2012-2016 is 34.6 % smaller. However, not all WF components reduce by the same magnitude. WF_g and WF_{bc} have reduced by more than one third between the two periods (-35.8 % and -39.4 %, respectively), while WF_{bi} has reduced by 14.4 %. To explain the decreasing trend in WF , the main contributing factors (see Sect. 2.1.3) – simulated yield (Y_s), crop water use (CWU), and yield scaling factor (S) – are analysed with the Mann–Kendall trend test (Hussain and Mahmud, 2019). This test detects significant increasing trends in S (+56.1 % since 1986; $p = 1.35 \times 10^{-14}$) and CWU (+0.1 % since 1986; $p = 5.90 \times 10^{-3}$), and no significant trend in Y_s ($p = 0.29$). Subsequent correlation analysis shows that WF significantly correlates only with S ($r = -0.97$, $t = -20.64$) and CWU ($r = -0.51$, $t = -3.19$). Hence, the reduction in WF can be mainly attributed to the increase in S , which is a factor that reflects external developments that cannot be modelled with ACEA (see Sect. 2.1.4). Once detrended, WF correlates significantly only with Y_s ($r = -0.73$; $t = -5.69$), and thus the interannual variations in WF are mainly driven by crop response to climatic variability reflected in Y_s . For example, the WF peaks around 1988 and 2012 (see Fig. 5) are likely due to extreme La Nina-driven droughts in major maize producing areas which caused substantial drops in crop yields (Iizumi et al., 2014; Rippey, 2015). A summary of global annual WF s and main contributing factors during 1986-2016 is provided in Table S3.

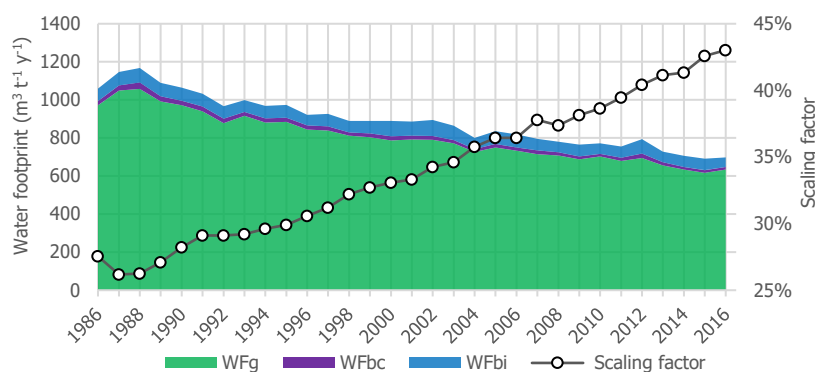


Figure 5: Global trends in average unit water footprints of maize (g - green, bc - blue from capillary rise, bi - blue from irrigation) in $m^3 t^{-1} y^{-1}$ and yield scaling factors from 1986 to 2016.

All major maize producing areas show a smaller unit WF of maize (i.e. increase in crop water productivity) in 2012-2016 compared to 1986-1990 (see Fig. 6). The regions with the largest WF reductions are Melanesia (-72.0 %), Southern Africa (-65.2 %), and South-eastern Asia (-59.9 %), which indicates substantial increases in their maize yields. On the other hand, the regions with the smallest reductions are Western Europe (-19.7 %) and Western Africa (-22.8 %). In the case of Western Europe, this is a result of already small WF in 1986-1990 ($518.4 m^3 t^{-1} y^{-1}$), and thus there was a low potential for WF reduction. In the case of Western Africa, there was a high reduction potential, but it was barely realised likely due to underlying socio-economic limitations (Smale et al., 2011).

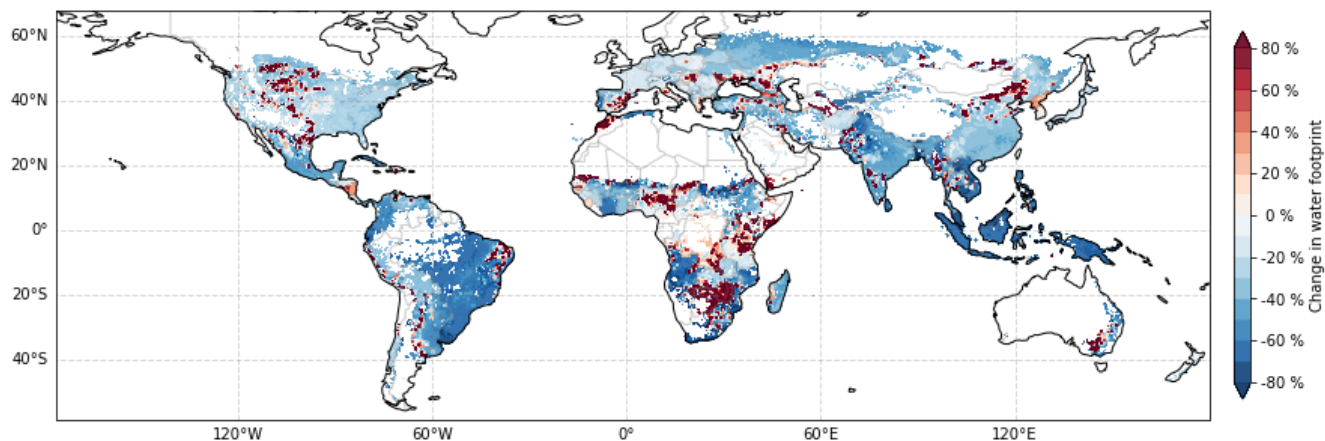


Figure 6: Relative change of unit water footprint of maize from the average of 1986-1990 to the average of 2012-2016 at 5 x 5 arc minute resolution.

At the national scale, countries that together account for 95 % of global maize production show a 32.9 % smaller unit *WF* of maize in 2012-2016 compared to 1986-1990 (see Fig. 7). Reductions of more than 50 % are in Brazil, Indonesia, South Africa, the Philippines, Vietnam, Pakistan, and Paraguay (see Table S2). These countries mostly rely on rainfed systems, and thus the *WF* reduction is mainly due to a smaller WF_g . On the other hand, there are three countries with a *WF* increase: +10.0 % in the Democratic Republic of Congo, +13.1 % in Kenya, and +33.1 % in the Democratic People's Republic of Korea. In total, these three countries produce only 0.77 % of maize globally.

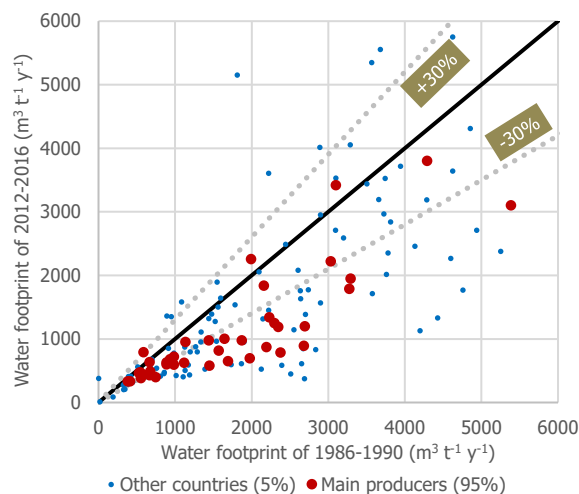


Figure 7: Comparison of the national unit water footprints of maize ($m^3 t^{-1} y^{-1}$) between the average of 1986-1990 and the average of 2012-2016. The black line represents no change and the grey dotted lines show +30 % and -30 % changes in unit water footprint.

The global *WF* of maize production has increased by 48.8 % since 1986 peaking at $762.9 \times 10^9 m^3 y^{-1}$ in 2016 (see Fig. 8). This increase differs among rainfed and irrigated systems. In rainfed systems, the consumption of green water and blue water from capillary rise have increased by 36.3 % and 33.8%, respectively. In irrigated systems, the consumption of green water and blue water from irrigation have increased by 114.4 % and 76.4%, respectively. The Mann-Kendall trend test detects



295

significant increasing trends in the two main contributing factors to the global WF of maize production: rainfed harvested area (+36.7 % since 1986; $p = 2.48 \times 10^{-8}$) and irrigated harvested area (+110.0 % since 1986; $p = 1.55 \times 10^{-14}$). Subsequent correlation analysis shows significant correlation with both factors ($r = 0.98$ each). Hence, the expansion of maize cropland increases global maize water consumption despite the reduction in unit *WF*. The detrended WF of maize production correlate significantly with the detrended harvested areas (rainfed $r = 0.95$; irrigated $r = 0.88$), which means that historical changes in maize cropland are responsible for its interannual variations.

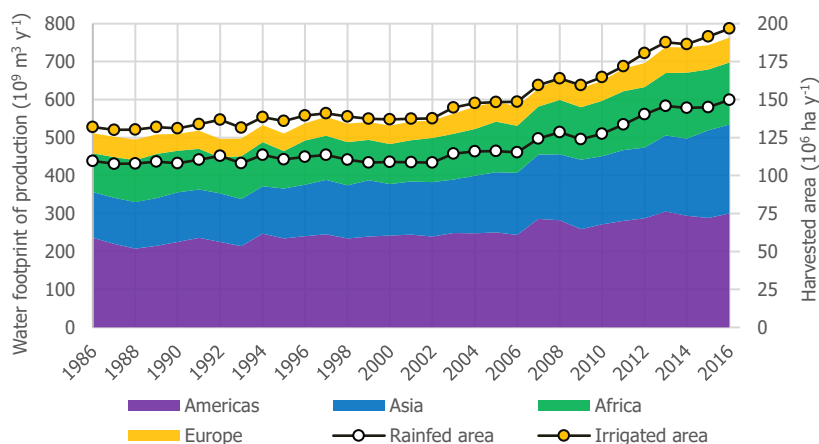


Figure 8: Regional trends in the water footprints of maize production ($10^9 \text{ m}^3 \text{ y}^{-1}$) and harvested areas (10^6 ha y^{-1}) from 1986 to 2016. Oceania is not shown due to its negligible contribution.

300

Most of the maize cropland expansion has occurred in Asia and Africa (+81.6 % and +76.5 %, respectively), which led to substantial increases in the WFs of maize production (+94.4 % and +60.2 %). At the same time, Americas and Europe have also increased their WFs of production (+27.1 % and +24 %), but the cropland expanded moderately (+25.7 % and +15.4 %). One of the main reasons behind a larger increase in WFs of production than in harvested areas lies in the substantial expansion of irrigated systems. They have a larger *CWU* than rainfed systems (+14 % on average), and hence the regions with a rapid expansion of them, such as +175.9 % in Asia (compared to +37.1 % in rainfed systems), experience an increase in the average *CWU*. As a result, the share of irrigated maize in the global WF of maize production has increased from 19.1% in 1986 to 26.0% in 2016.

305

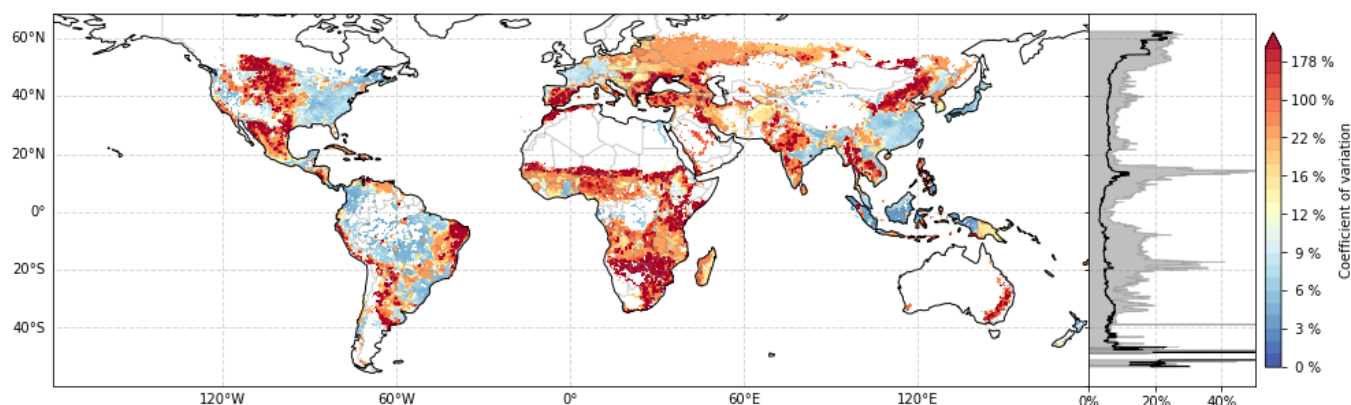
3.3 Interannual variability in maize water footprints

The interannual variability in unit *WF* of maize is analysed using the coefficient of variation (*CV*) estimated for the detrended values during 1986-2016. The global average *CV* for this period is 21.3 %: 8.4 % in irrigated systems and 28.8 % in rainfed systems. The variability in rainfed systems differs around the world depending on maize yield response to water availability. For instance, the average *CV* of regions with capillary rise contribution is 14.7 %, while many arid parts of Sub-Saharan Africa that completely rely on rainfall have *CV* values higher than 100 % (see Fig. 9). On the other hand, the *WF* variability in irrigated systems is generally low in all regions as also suggested by previous studies (Kucharik and

310



315 Ramankutty, 2005; Osborne and Wheeler, 2013). The interannual variability also depends on the level of agricultural development and socio-economic stability (as reflected by yield scaling factors). In Western Europe, the average *CV* is 9.5 % despite being mostly rainfed, while in Central Asia the average *CV* is 22.4 % despite being 100 % irrigated. The *CV* values of other regions are listed in Table 2.



320 **Figure 9: Coefficient of variation of the detrended unit water footprints of maize during 1986-2016 at 5 x 5 arc minute resolution. The grey area in the side chart represents the median of all data points along the respective latitude and the black line is the 10 % percentile of them.**

4 Discussion

4.1 Comparison of results with literature

4.1.1 Average maize water footprints around 2000

325 Three previous studies have estimated maize WFs at the global scale with a distinction between green and blue water (see Table 3). All three focus on the period around the year 2000, and thus we average our results for a similar period to make the comparison (1996-2005). Both our and previous studies agree on the dominant role of green water in the global average unit *WF* of maize (~90%). However, previous studies show larger unit *WF* estimates compared to the present study: +24 % by Siebert and Döll (2010), +20 % by Mekonnen and Hoekstra (2011), and +12 % by Tuninetti et al. (2015). These *WF* differences are likely caused by different methods applied to estimate *CWU* since the differences in the global average crop yields are relatively small (-4 % to +12 %).

Table 3: Comparison of ACEA results for maize with other global gridded studies. Numbers in brackets indicate the difference compared to the results of ACEA.

Source	Water footprint calculation approach	Shallow groundwater	Averaging period	Crop yield [$t^1 ha^{-1}$]		Average unit water footprint [$m^3 t^{-1} y^{-1}$]		
				Rainfed	Irrigated	Green	Blue	Total
Our study	Process-based and water-driven model in growing degree days with incorporated green-blue separation	Considered	1996-2005 (with trend)	4.3	5.4	792	88	880



Siebert and Döll (2010)	Daily soil water balance model and crop coefficient approach with green-blue separation in post-processing	Not Considered	1998-2002 (with trend)	4.1 (-4%)	5.7 (+6%)	969 (+22%)	120 (+36%)	1089 (+24%)
Mekonnen and Hoekstra (2011)	Similar to Siebert and Döll (2010), but for one representative year	Not Considered	1996-2005 (no trend)	4.1 (-4%)	6 (+12%)	947 (+20%)	81 (-8%)	1028 (+17%)
Tuinetti et al. (2015)	Crop coefficient approach with evapotranspiration and crop yields from literature	Not Considered	1996-2005 (with trend)	-	-	886* (+12%)	47* (-47%)	933 (+6%)

* approximate estimates from the reported total water consumption as unit water footprint components were not explicitly provided.

- 335 The study by Siebert and Döll (2010) estimates a larger green (+22 %) and blue *CWU* (+36 %) compared to our study. One of the reasons for these higher estimates is that the authors assume a pre-defined root depth and canopy development (linear interpolation between crop factors in the initial, mid and late season stages), whereas in our study both of them are driven by daily temperature and water availability. The latter is particularly important since water stress leads to stomatal closure, which reduces crop transpiration. Therefore, crop transpiration and root water uptake in ACEA are likely to be smaller
- 340 leading to reduction in *CWU* values. There are several other reasons for differences in *CWU* between the two studies, but to what degree they explain the lower estimates in ACEA is difficult to answer. Siebert and Döll (2010) consider a constant growing season duration using the crop calendar based on the year 2000, while in our model the growing season duration is temperature-dependent and the crop calendar is a composite of multiple recent data sources (see Sect. 2.1.4). Consequently, crop calendar days differ among the two studies leading to different daily weather conditions and growing season durations.
- 345 This results in different ET rates accumulated over the crop cycle, and hence different *CWU* values. Moreover, the authors estimate green and blue *CWU* in post-processing, which is less accurate than tracing it directly during the modelling as in ACEA (see Sect. 2.1.2). The authors also cover a shorter historical period and use two older input datasets: climatic data that directly affects water availability and ET rates, and harvested area data that results in different sizes of rainfed and irrigated systems, which are important in the global averaging of results.
- 350 The study by Mekonnen and Hoekstra (2011) also shows a larger green *CWU* (+20 %) but a blue *CWU* is smaller (-8 %). The authors use a relatively similar modelling approach as Siebert and Döll (2010), but they simulate only one representative year, which neglects the interannual variability in climatic variables as well as trends in agricultural development and harvested areas. Therefore, *CWU* estimates do not capture years with abnormal weather (wet, dry, cold, warm).
- 355 Tuninetti et al. (2015) also report a larger green *CWU* (+12 %) but smaller blue *CWU* (-47 %). The authors do not model the reference evapotranspiration and crop yields (as the other studies do) but take them from literature instead. Moreover, they equalize blue *CWU* to irrigation supply which is calculated using independent data sources of different temporal and spatial resolutions.
- Due to limitations on data availability, we only compare our national unit *WF* estimates to Mekonnen and Hoekstra (2011). Both studies correlate well ($r = 0.95$) as shown in Fig. 10. Among 148 considered countries, 52 have a unit *WF* difference of
- 360 more than 30 % and countries that produce 95 % of maize globally have on average the difference of 15.3 %.

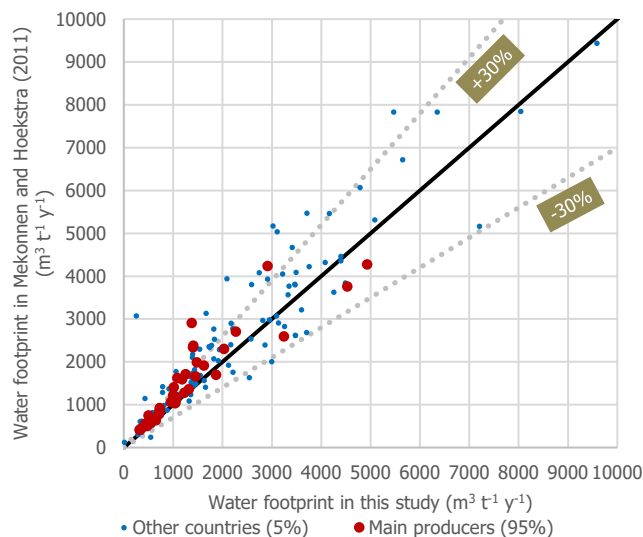


Figure 10: National comparison of unit water footprints of maize ($\text{m}^3 \text{t}^{-1} \text{y}^{-1}$) around 2000 with Mekonnen and Hoekstra (2011). The black line represents no difference and the grey dotted lines show +30 % and -30 % differences in unit water footprint.

The methodological differences among these three studies also lead to different estimates of the global WFs of maize
365 production. Compared to our study, Siebert and Döll (2010) and Mekonnen and Hoekstra (2011) show similar directions and
magnitudes of differences and report 17-19 % larger estimates (37-40 % larger green but 43-60 % smaller blue), while
Tuninetti et al. (2015) report a 50 % larger estimate (85 % larger green but 68 % smaller blue).

4.1.2 Historical trends and variability in maize water footprints

We are not aware of any other study that simulates maize WFs for the same time period as our study. However, the
370 comparisons of WFs and main contributing factors can be done for a few historical periods. For example, the recent
literature review of 70 related studies (during 2002-2018) by Feng et al. (2021) reports a global average unit *WF* of maize of
 $730 \text{ m}^3 \text{t}^{-1} \text{y}^{-1}$ with a *CV* of 15.9 %. This aligns well with our estimate of $723.2 \text{ m}^3 \text{t}^{-1} \text{y}^{-1}$ with a *CV* of 21.3%. Approximate
comparisons can be also done for maize yield gaps. Three studies estimate the global yield gaps around 2000 in a range of
50-64 % (Licker et al., 2010; Mueller et al., 2012; Neumann et al., 2010). Our estimate of the water-limited yield gap for
375 1996-2005 in ACEA is 67%. Two more recent studies report yield gaps around 2010 for several locations in different
regions (Hoffmann et al., 2018; Edreira et al., 2018). Their estimates show similarities to our study (calculated for 2012-
2016): 80 % yield gap in Sub-Saharan Africa (75 % in ACEA), 20 % in Northern America (30.5 % in ACEA), and 38 % in
East Asia (55.7 % in ACEA). More pessimistic results of our study are likely due to differences in yield-limiting factors and
cropland extents.



380 4.2 Strengths and weaknesses of ACEA

4.2.1 Advancing crop water productivity research

ACEA is the first process-based GGCM that can trace the fluxes of green water, blue water from capillary rise, and blue water from irrigation within the soil profile on a daily time step. This allows to accurately distinguish between green and blue crop water productivity (Hoekstra, 2019). To demonstrate usefulness of this distinction, we highlight the importance of accounting blue water from capillary rise as its contribution to the national WF of maize production can amount to 25 % (see Sect. 3.1). Furthermore, the open-source nature and advanced functionality of ACEA facilitates simulations of various alternative management packages (e.g. field management practices, irrigation methods and strategies). This allows studying responses of crop water productivity to various environmental and managerial changes.

4.2.2 Uncertainties in global crop modelling

390 Global gridded crop modelling is a complex process that contains several uncertainties (Folberth et al., 2019) and ACEA is not an exception. Most of uncertainties originate from spatial and temporal resolutions of input datasets rather than from the model itself. In our study, we model maize production at 30 x 30 arc minute resolution meaning that input datasets with finer resolutions have to be upscaled, such as soil characteristics and shallow groundwater levels (see Sect. 2.2). Then, we downscale simulation results to 5 x 5 arc minute resolution, which leads to uncertainty in crop yields and *CWU* estimates as they do not reflect the exact environmental conditions in each 5 x 5 arc minute grid cell. Alternatively, ACEA can be run at 5 x 5 arc minutes but this is not feasible for our study due to high computational requirements and input data limitations (see Sect. 2.2).

Next, maize crop parameters are based on a single cultivar calibrated for several agro-climatic conditions by FAO (Hsiao et al., 2009). Therefore, the regional and historical differences in crop genetics such as water productivity, root depth, and abiotic stress responses are not considered. Moreover, the lack of subnational data needed to generate reliable crop calendars results in a poor representation of spatial variability in planting and harvest dates. Thus, the start and duration of growing seasons might be miscalculated which, again, leads to uncertainties in simulated crop yields and *CWU*. We also assume the same soil moisture-based rule for irrigation application in all grid cells. In reality, farmers decide when and how much to irrigate based on site-specific conditions such as access to water and technological inputs. Note that the current version of ACEA does not consider chemical cycles between a crop and the environment. Therefore, the biomass accumulation stresses from water salinity and insufficient nutrient intake are not simulated but captured in the national yield scaling factors (see Sect. 2.1.4).

The post-processing of results also contains uncertainties. In particular, the geographical extent of maize production plays an important role during spatial averaging. To our knowledge, we make the first-ever attempt to temporally extrapolate maize harvested areas (see Sect. S1.6); hence, our gridded estimates for rainfed and irrigated systems are only approximate. These uncertainties are particularly relevant when zooming to smaller geographical scales (e.g. analysis of small countries).



4.2.3 Future prospects

In this paper, we apply ACEA to study the historic and current state of maize WFs in the world. However, maize covers only a fraction of overall crop production globally, and hence WFs of other crops should be analysed to provide a complete
415 overview of developments in crop water productivity and water consumption worldwide. Furthermore, regional impacts of crop production on ecosystems and freshwater resources can only be assessed by relating the total WF of production (agricultural, industrial, and domestic) to maximum sustainable levels within a given geographical unit (Bunsen et al., 2021; Hoekstra et al., 2012b; Liu et al., 2017; Hogeboom et al., 2020). WFs in crop growing areas that already overshoot (or soon to overshoot) these levels can be further assessed in ACEA to propose potential measures of WF reduction, such as more
420 efficient irrigation and field management (Chukalla et al., 2015, 2017; Campbell et al., 2017; Nouri et al., 2019) or change of cropping patterns (Chouchane et al., 2020).

5 Conclusions

This study introduces a new process-based global gridded crop model – AquaCrop-Earth@lternatives (ACEA) – that can simulate crop water productivity at high spatial and temporal resolutions. The main novelty of ACEA lies in its ability to
425 trace fluxes of green water, blue water from capillary rise, and blue water from irrigation within the soil profile on a daily time step. This allows to estimate the precise contribution of these three water types to the final crop WF.

We apply ACEA to analyse global maize WFs during 1986-2016 at 5 x 5 arc minute resolution. Our results show that, in 2012-2016, the global average unit WF of maize is $723.2 \text{ m}^3 \text{ t}^{-1} \text{ y}^{-1}$ with a dominant role of green water (89.5 % of total), followed by blue water from irrigation (8.3%), and blue water from capillary rise (2.2%). Despite being minor at the global
430 scale, the role of blue WF from capillary rise becomes substantial when zooming to regions with a wide presence of shallow groundwater tables. We also find that rainfed areas with capillary rise contribution have a twice lower interannual variability in unit WF (CV of 14.7%) than rainfed areas without such contribution (28.8%). However, the lowest interannual variability is found in irrigated areas (8.4%).

Spatial and temporal patterns in maize unit WFs are mostly determined by crop yields. Regions with small yield gaps and/or
435 favourable climate conditions (e.g. low ET rates, sufficient rainfall) have a small unit WF and its interannual variation, such as Western Europe and Northern America ($\text{WF} < 500 \text{ m}^3 \text{ t}^{-1} \text{ y}^{-1}$, $\text{CV} < 15\%$). Regions with large yield gaps have opposite outcomes, such as Middle and Eastern Africa ($\text{WF} > 2500 \text{ m}^3 \text{ t}^{-1} \text{ y}^{-1}$, $\text{CV} > 40\%$). Consequently, these regions have potential to substantially reduce their unit WFs of maize, and hence to improve local food and water security.

Our results also reveal a rebound effect of global crop water productivity gains: the average unit WF of maize has decreased
440 by one third since 1986, but the WF of maize production has increased by almost one half reaching $762.9 \times 10^9 \text{ m}^3 \text{ y}^{-1}$ in 2016. This dynamic is mainly driven by two factors: decreasing yield gaps and expanding croplands. Since decreasing yield gaps are insufficient to satisfy the global maize demand, farmers started expanding both rainfed and irrigated croplands.



Consequently, more and more maize is cultivated which increases maize's water consumption worldwide (mostly in Asia and Africa).

445 As maize production consumes more water than ever before, it is important to evaluate other crops in ACEA too. This would advance the understanding of temporal and spatial patterns in WFs of crops as well as allow assessing the pressure of crop production on ecosystems and freshwater resources worldwide.

Code and data availability

450 Input and output datasets that are not provided in the paper or the supplement as well as Python and MATLAB scripts can be provided by the corresponding author upon request.

Author contributions

OM, JFS, and MJB designed the study and the model. OM wrote the code and carried out the simulations. All authors did the analysis. OM prepared the manuscript with contributions from all co-authors.

Competing interests

455 The authors declare that they have no conflict of interest.

Acknowledgements

460 We dedicate our study to Prof. Arjen Y. Hoekstra (1967-2019) who initiated this research but unfortunately passed away before it was published. All authors were supported by the European Research Council (ERC) under the European Union's Horizon 2020 research and innovation programme (Earth@lternatives project, grant agreement No 834716). The ACEA simulations were mostly carried out using the Dutch national e-infrastructure with the support of SURF Cooperative.

References

- Allen, R. G., Pereira, L. S., Raes, D., and Smith, M.: Crop evapotranspiration: guidelines for computing crop water requirements - FAO irrigation and drainage paper 56, Food and Agriculture Organization of the United Nations, Rome, 300 pp., 1998.
- 465 Amante, C.: ETOPO1 1 Arc-Minute Global Relief Model: Procedures, Data Sources and Analysis, <https://doi.org/10.7289/V5C8276M>, 2009.



- Andarzian, B., Bannayan, M., Steduto, P., Mazraeh, H., Barati, M. E., Barati, M. A., and Rahnama, A.: Validation and testing of the AquaCrop model under full and deficit irrigated wheat production in Iran, *Agricultural Water Management*, 100, 1–8, <https://doi.org/10.1016/j.agwat.2011.08.023>, 2011.
- 470 QGIS: <https://qgis.org/en/site/>, last access: 16 June 2021.
- UNSD: <https://unstats.un.org/unsd/methodology/m49/>, last access: 3 June 2021.
- Araya, A., Kisekka, I., and Holman, J.: Evaluating deficit irrigation management strategies for grain sorghum using AquaCrop, *Irrig Sci*, 34, 465–481, <https://doi.org/10.1007/s00271-016-0515-7>, 2016.
- Brown, C. E.: *Applied multivariate statistics in geohydrology and related sciences*, Springer, Berlin; New York, 1998.
- 475 Bunsen, J., Berger, M., and Finkbeiner, M.: Planetary boundaries for water – A review, *Ecological Indicators*, 121, 107022, <https://doi.org/10.1016/j.ecolind.2020.107022>, 2021.
- Campbell, B. M., Beare, D. J., Bennett, E. M., Hall-Spencer, J. M., Ingram, J. S. I., Jaramillo, F., Ortiz, R., Ramankutty, N., Sayer, J. A., and Shindell, D.: Agriculture production as a major driver of the Earth system exceeding planetary boundaries, *E&S*, 22, art8, <https://doi.org/10.5751/ES-09595-220408>, 2017.
- 480 Chapagain, A. K. and Hoekstra, A. Y.: The blue, green and grey water footprint of rice from production and consumption perspectives, *Ecological Economics*, 70, 749–758, <https://doi.org/10.1016/j.ecolecon.2010.11.012>, 2011.
- Chouchane, H., Krol, M. S., and Hoekstra, A. Y.: Changing global cropping patterns to minimize national blue water scarcity, *Hydrol. Earth Syst. Sci.*, 24, 3015–3031, <https://doi.org/10.5194/hess-24-3015-2020>, 2020.
- Chukalla, A. D., Krol, M. S., and Hoekstra, A. Y.: Green and blue water footprint reduction in irrigated agriculture: effect of irrigation techniques, irrigation strategies and mulching, *Hydrol. Earth Syst. Sci.*, 19, 4877–4891, <https://doi.org/10.5194/hess-19-4877-2015>, 2015.
- 485 Chukalla, A. D., Krol, M. S., and Hoekstra, A. Y.: Marginal cost curves for water footprint reduction in irrigated agriculture: guiding a cost-effective reduction of crop water consumption to a permit or benchmark level, *Hydrol. Earth Syst. Sci.*, 21, 3507–3524, <https://doi.org/10.5194/hess-21-3507-2017>, 2017.
- 490 Edreira, J. I. R., Guilpart, N., Sadras, V., Cassman, K. G., van Ittersum, M. K., Schils, R. L. M., and Grassini, P.: Water productivity of rainfed maize and wheat: A local to global perspective, *Agricultural and Forest Meteorology*, 259, 364–373, <https://doi.org/10.1016/j.agrformet.2018.05.019>, 2018.
- Fan, Y., Li, H., and Miguez-Macho, G.: Global Patterns of Groundwater Table Depth, *Science*, 339, 940–943, <https://doi.org/10.1126/science.1229881>, 2013.
- 495 FAOSTAT: <http://www.fao.org/faostat>, last access: 15 May 2021.
- Feng, B., Zhuo, L., Xie, D., Mao, Y., Gao, J., Xie, P., and Wu, P.: A quantitative review of water footprint accounting and simulation for crop production based on publications during 2002–2018, *Ecological Indicators*, 120, 106962, <https://doi.org/10.1016/j.ecolind.2020.106962>, 2021.
- Folberth, C., Elliott, J., Müller, C., Balkovič, J., Chryssanthacopoulos, J., Izaurrealde, R. C., Jones, C. D., Khabarov, N., Liu, W., Reddy, A., Schmid, E., Skalský, R., Yang, H., Arneth, A., Ciais, P., Deryng, D., Lawrence, P. J., Olin, S., Pugh, T. A.
- 500



- M., Ruane, A. C., and Wang, X.: Parameterization-induced uncertainties and impacts of crop management harmonization in a global gridded crop model ensemble, *PLoS ONE*, 14, e0221862, <https://doi.org/10.1371/journal.pone.0221862>, 2019.
- Foster, T., Brozović, N., Butler, A. P., Neale, C. M. U., Raes, D., Steduto, P., Fereres, E., and Hsiao, T. C.: AquaCrop-OS: An open source version of FAO's crop water productivity model, *Agricultural Water Management*, 181, 18–22, <https://doi.org/10.1016/j.agwat.2016.11.015>, 2017.
- 505 Franke, J. A., Müller, C., Elliott, J., Ruane, A. C., Jägermeyr, J., Snyder, A., Dury, M., Falloon, P. D., Folberth, C., François, L., Hank, T., Izaurralde, R. C., Jacquemin, I., Jones, C., Li, M., Liu, W., Olin, S., Phillips, M., Pugh, T. A. M., Reddy, A., Williams, K., Wang, Z., Zabel, F., and Moyer, E. J.: The GGCM Phase 2 emulators: global gridded crop model responses to changes in CO₂, temperature, water, and nitrogen (version 1.0), *Geosci. Model Dev.*, 13, 3995–4018, <https://doi.org/10.5194/gmd-13-3995-2020>, 2020.
- 510 Giordano, M. A., Rijsberman, F. R., Saleth, R. M., and International Water Management Institute (Eds.): *More crop per drop: revisiting a research paradigm: results and synthesis of IWMI's research, 1996-2005*, IWA Pub, London, UK, 273 pp., 2006.
- Greaves, G. and Wang, Y.-M.: Assessment of FAO AquaCrop Model for Simulating Maize Growth and Productivity under Deficit Irrigation in a Tropical Environment, *Water*, 8, 557, <https://doi.org/10.3390/w8120557>, 2016.
- 515 Greve, P., Kahil, T., Mochizuki, J., Schinko, T., Satoh, Y., Burek, P., Fischer, G., Tramberend, S., Burtscher, R., Langan, S., and Wada, Y.: Global assessment of water challenges under uncertainty in water scarcity projections, *Nat. Sustain.*, 1, 486–494, <https://doi.org/10.1038/s41893-018-0134-9>, 2018.
- Han, C., Zhang, B., Chen, H., Liu, Y., and Wei, Z.: Novel approach of upscaling the FAO AquaCrop model into regional scale by using distributed crop parameters derived from remote sensing data, *Agricultural Water Management*, 240, 106288, <https://doi.org/10.1016/j.agwat.2020.106288>, 2020.
- 520 Hoekstra, A. Y. (Ed.): *The water footprint assessment manual: setting the global standard*, Earthscan, London ; Washington, DC, 203 pp., 2011.
- Hoekstra, A. Y.: Green-blue water accounting in a soil water balance, *Advances in Water Resources*, 129, 112–117, <https://doi.org/10.1016/j.advwatres.2019.05.012>, 2019.
- 525 Hoekstra, A. Y. and Mekonnen, M. M.: The water footprint of humanity, *Proceedings of the National Academy of Sciences*, 109, 3232–3237, <https://doi.org/10.1073/pnas.1109936109>, 2012.
- Hoekstra, A. Y., Booij, M. J., Hunink, J. C., and Meijer, K. S.: Blue water footprint of agriculture, industry, households and water management in the Netherlands: An exploration of using the Netherlands Hydrological Instrument, *Unesco-IHE Institute for Water Education*, Delft, the Netherlands, 2012a.
- 530 Hoekstra, A. Y., Mekonnen, M. M., Chapagain, A. K., Mathews, R. E., and Richter, B. D.: Global Monthly Water Scarcity: Blue Water Footprints versus Blue Water Availability, *PLoS ONE*, 7, e32688, <https://doi.org/10.1371/journal.pone.0032688>, 2012b.



- Hoffmann, M. P., Haakana, M., Asseng, S., Höhn, J. G., Palosuo, T., Ruiz-Ramos, M., Fronzek, S., Ewert, F., Gaiser, T.,
535 Kassie, B. T., Paff, K., Rezaei, E. E., Rodríguez, A., Semenov, M., Srivastava, A. K., Stratonovitch, P., Tao, F., Chen, Y.,
and Rötter, R. P.: How does inter-annual variability of attainable yield affect the magnitude of yield gaps for wheat and
maize? An analysis at ten sites, *Agricultural Systems*, 159, 199–208, <https://doi.org/10.1016/j.agry.2017.03.012>, 2018.
- Hogeboom, R. J., Bruin, D., Schyns, J. F., Krol, M. S., and Hoekstra, A. Y.: Capping Human Water Footprints in the
World's River Basins, *Earth's Future*, 8, <https://doi.org/10.1029/2019EF001363>, 2020.
- 540 Hsiao, T. C., Heng, L., Steduto, P., Rojas-Lara, B., Raes, D., and Fereres, E.: AquaCrop-The FAO Crop Model to Simulate
Yield Response to Water: III. Parameterization and Testing for Maize, *Agron. J.*, 101, 448–459,
<https://doi.org/10.2134/agronj2008.0218s>, 2009.
- Huang, J., Scherer, L., Lan, K., Chen, F., and Thorp, K. R.: Advancing the application of a model-independent open-source
geospatial tool for national-scale spatiotemporal simulations, *Environmental Modelling & Software*, 119, 374–378,
545 <https://doi.org/10.1016/j.envsoft.2019.07.003>, 2019.
- Hussain, Md. and Mahmud, I.: pyMannKendall: a python package for non parametric Mann Kendall family of trend tests.,
JOSS, 4, 1556, <https://doi.org/10.21105/joss.01556>, 2019.
- Iizumi, T., Luo, J.-J., Challinor, A. J., Sakurai, G., Yokozawa, M., Sakuma, H., Brown, M. E., and Yamagata, T.: Impacts of
El Niño Southern Oscillation on the global yields of major crops, *Nat Commun*, 5, 3712,
550 <https://doi.org/10.1038/ncomms4712>, 2014.
- ISIMIP: <https://protocol.isimip.org/protocol/ISIMIP3b/agriculture.html>, last access: 14 September 2020.
- Jägermeyr, J., Gerten, D., Heinke, J., Schaphoff, S., Kummu, M., and Lucht, W.: Water savings potentials of irrigation
systems: global simulation of processes and linkages, *Hydrol. Earth Syst. Sci.*, 19, 3073–3091, <https://doi.org/10.5194/hess-19-3073-2015>, 2015.
- 555 Jaramillo, F. and Destouni, G.: Local flow regulation and irrigation raise global human water consumption and footprint,
Science, 350, 1248–1251, <https://doi.org/10.1126/science.aad1010>, 2015.
- Karandish, F. and Hoekstra, Arjen.: Informing National Food and Water Security Policy through Water Footprint
Assessment: the Case of Iran, *Water*, 9, 831, <https://doi.org/10.3390/w9110831>, 2017.
- Khoshravesh, M., Mostafazadeh-Fard, B., Heidarpour, M., and Kiani, A.-R.: AquaCrop model simulation under different
560 irrigation water and nitrogen strategies, 67, 232–238, <https://doi.org/10.2166/wst.2012.564>, 2013.
- Kucharik, C. J. and Ramankutty, N.: Trends and Variability in U.S. Corn Yields Over the Twentieth Century, 9, 1–29,
<https://doi.org/10.1175/EI098.1>, 2005.
- Lange, S.: WFDE5 over land merged with ERA5 over the ocean (W5E5) (1.0), <https://doi.org/10.5880/PIK.2019.023>, 2019.
- Licker, R., Johnston, M., Foley, J. A., Barford, C., Kucharik, C. J., Monfreda, C., and Ramankutty, N.: Mind the gap: how
565 do climate and agricultural management explain the ‘yield gap’ of croplands around the world?: Investigating drivers of
global crop yield patterns, 19, 769–782, <https://doi.org/10.1111/j.1466-8238.2010.00563.x>, 2010.



- Liu, J., Yang, H., Gosling, S. N., Kummu, M., Flörke, M., Pfister, S., Hanasaki, N., Wada, Y., Zhang, X., Zheng, C., Alcamo, J., and Oki, T.: Water scarcity assessments in the past, present, and future: REVIEW ON WATER SCARCITY ASSESSMENT, *Earth's Future*, 5, 545–559, <https://doi.org/10.1002/2016EF000518>, 2017.
- 570 Lorite, I. J., García-Vila, M., Santos, C., Ruiz-Ramos, M., and Fereres, E.: AquaData and AquaGIS: Two computer utilities for temporal and spatial simulations of water-limited yield with AquaCrop, *Computers and Electronics in Agriculture*, 96, 227–237, <https://doi.org/10.1016/j.compag.2013.05.010>, 2013.
- Lovarelli, D., Bacenetti, J., and Fiala, M.: Water Footprint of crop productions: A review, *Sci. Total Environ.*, 548, 236–251, <https://doi.org/10.1016/j.scitotenv.2016.01.022>, 2016.
- 575 Maniruzzaman, M., Talukder, M. S. U., Khan, M. H., Biswas, J. C., and Nemes, A.: Validation of the AquaCrop model for irrigated rice production under varied water regimes in Bangladesh, *Agricultural Water Management*, 159, 331–340, <https://doi.org/10.1016/j.agwat.2015.06.022>, 2015.
- McNider, R. T., Handyside, C., Doty, K., Ellenburg, W. L., Cruise, J. F., Christy, J. R., Moss, D., Sharda, V., Hoogenboom, G., and Caldwell, P.: An integrated crop and hydrologic modeling system to estimate hydrologic impacts of crop irrigation demands, *Environmental Modelling & Software*, 72, 341–355, <https://doi.org/10.1016/j.envsoft.2014.10.009>, 2015.
- 580 Mekonnen, M. M. and Hoekstra, A. Y.: A global and high-resolution assessment of the green, blue and grey water footprint of wheat, *Hydrol. Earth Syst. Sci.*, 14, 1259–1276, <https://doi.org/10.5194/hess-14-1259-2010>, 2010.
- Mekonnen, M. M. and Hoekstra, A. Y.: The green, blue and grey water footprint of crops and derived crop products, *Hydrol. Earth Syst. Sci.*, 15, 1577–1600, <https://doi.org/10.5194/hess-15-1577-2011>, 2011.
- 585 Mueller, N. D., Gerber, J. S., Johnston, M., Ray, D. K., Ramankutty, N., and Foley, J. A.: Closing yield gaps through nutrient and water management, *Nature*, 490, 254–257, <https://doi.org/10.1038/nature11420>, 2012.
- Müller, C., Elliott, J., Chryssanthacopoulos, J., Arneth, A., Balkovic, J., Ciais, P., Deryng, D., Folberth, C., Glotter, M., Hoek, S., Iizumi, T., Izaurrealde, R. C., Jones, C., Khabarov, N., Lawrence, P., Liu, W., Olin, S., Pugh, T. A. M., Ray, D. K., Reddy, A., Rosenzweig, C., Ruane, A. C., Sakurai, G., Schmid, E., Skalsky, R., Song, C. X., Wang, X., de Wit, A., and
- 590 Yang, H.: Global gridded crop model evaluation: benchmarking, skills, deficiencies and implications, *Geosci. Model Dev.*, 10, 1403–1422, <https://doi.org/10.5194/gmd-10-1403-2017>, 2017.
- Nachtergaele, F. O., Velthuisen, H. van, Verelst, L., Batjes, N. H., Dijkshoorn, J. A., Engelen, V. W. P. van, Fischer, G., Jones, A., Montanarella, L., Petri, M., Prieler, S., Teixeira, E., Wilberg, D., and Shi, X.: Harmonized World Soil Database (version 1.0), 2008.
- 595 Neumann, K., Verburg, P. H., Stehfest, E., and Müller, C.: The yield gap of global grain production: A spatial analysis, *Agricultural Systems*, 103, 316–326, <https://doi.org/10.1016/j.agsy.2010.02.004>, 2010.
- Nouri, H., Stokvis, B., Galindo, A., Blatchford, M., and Hoekstra, A. Y.: Water scarcity alleviation through water footprint reduction in agriculture: The effect of soil mulching and drip irrigation, *Science of The Total Environment*, 653, 241–252, <https://doi.org/10.1016/j.scitotenv.2018.10.311>, 2019.



- 600 Osborne, T. M. and Wheeler, T. R.: Evidence for a climate signal in trends of global crop yield variability over the past 50 years, *Environ. Res. Lett.*, 8, 024001, <https://doi.org/10.1088/1748-9326/8/2/024001>, 2013.
- Portmann, F. T., Siebert, S., and Döll, P.: MIRCA2000-Global monthly irrigated and rainfed crop areas around the year 2000: A new high-resolution data set for agricultural and hydrological modeling: MONTHLY IRRIGATED AND RAINFED CROP AREAS, *Global Biogeochem. Cycles*, 24, n/a-n/a, <https://doi.org/10.1029/2008GB003435>, 2010.
- 605 Raes, D., Steduto, P., Hsiao, T. C., and Fereres, E.: AquaCrop-The FAO Crop Model to Simulate Yield Response to Water: II. Main Algorithms and Software Description, *Agron. J.*, 101, <https://doi.org/10.2134/agronj2008.0140s>, 2009.
- Raes, D., Steduto, P., Hsiao, T. C., and Fereres, E.: AquaCrop Version 6.0 - 6.1: Reference manual (Annexes), Rome, 2018.
- Rippey, B. R.: The U.S. drought of 2012, *Weather and Climate Extremes*, 10, 57–64, <https://doi.org/10.1016/j.wace.2015.10.004>, 2015.
- 610 Rosenzweig, C., Elliott, J., Deryng, D., Ruane, A. C., Müller, C., Arneth, A., Boote, K. J., Folberth, C., Glotter, M., Khabarov, N., Neumann, K., Piontek, F., Pugh, T. A. M., Schmid, E., Stehfest, E., Yang, H., and Jones, J. W.: Assessing agricultural risks of climate change in the 21st century in a global gridded crop model intercomparison, *Proc Natl Acad Sci USA*, 111, 3268–3273, <https://doi.org/10.1073/pnas.1222463110>, 2014.
- Ruane, A., Antle, J., Elliott, J., Folberth, C., Hoogenboom, G., Mason-D’Croz, D., Müller, C., Porter, C., Phillips, M.,
- 615 Raymundo, R., Sands, R., Valdivia, R., White, J., Wiebe, K., and Rosenzweig, C.: Biophysical and economic implications for agriculture of +1.5° and +2.0°C global warming using AgMIP Coordinated Global and Regional Assessments, *Clim. Res.*, 76, 17–39, <https://doi.org/10.3354/cr01520>, 2018.
- Saxton, K. E. and Rawls, W. J.: Soil Water Characteristic Estimates by Texture and Organic Matter for Hydrologic Solutions, *Soil Sci. Soc. Am. J.*, 70, 1569–1578, <https://doi.org/10.2136/sssaj2005.0117>, 2006.
- 620 Schyns, J. F., Hoekstra, A. Y., Booij, M. J., Hogeboom, R. J., and Mekonnen, M. M.: Limits to the world’s green water resources for food, feed, fiber, timber, and bioenergy, *Proc Natl Acad Sci USA*, 116, 4893–4898, <https://doi.org/10.1073/pnas.1817380116>, 2019.
- Siebert, S. and Döll, P.: Quantifying blue and green virtual water contents in global crop production as well as potential production losses without irrigation, *Journal of Hydrology*, 384, 198–217, <https://doi.org/10.1016/j.jhydrol.2009.07.031>,
- 625 2010.
- Smale, M., Byerlee, D., and Jayne, T.: Maize Revolutions in Sub-Saharan Africa, The World Bank, <https://doi.org/10.1596/1813-9450-5659>, 2011.
- Steduto, P., Hsiao, T. C., Raes, D., and Fereres, E.: AquaCrop-The FAO Crop Model to Simulate Yield Response to Water: I. Concepts and Underlying Principles, *Agron. J.*, 101, 426–437, <https://doi.org/10.2134/agronj2008.0139s>, 2009.
- 630 Tuninetti, M., Tamea, S., D’Odorico, P., Laio, F., and Ridolfi, L.: Global sensitivity of high-resolution estimates of crop water footprint, *Water Resour. Res.*, 51, 8257–8272, <https://doi.org/10.1002/2015WR017148>, 2015.



- Vanuytrecht, E., Raes, D., Steduto, P., Hsiao, T. C., Fereres, E., Heng, L. K., Garcia Vila, M., and Mejias Moreno, P.: AquaCrop: FAO's crop water productivity and yield response model, *Environmental Modelling & Software*, 62, 351–360, <https://doi.org/10.1016/j.envsoft.2014.08.005>, 2014.
- 635 Wada, Y. and Bierkens, M. F. P.: Sustainability of global water use: past reconstruction and future projections, *Environ. Res. Lett.*, 9, 104003, <https://doi.org/10.1088/1748-9326/9/10/104003>, 2014.
- Wang, X., Müller, C., Elliot, J., Mueller, N. D., Ciais, P., Jägermeyr, J., Gerber, J., Dumas, P., Wang, C., Yang, H., Li, L., Deryng, D., Folberth, C., Liu, W., Makowski, D., Olin, S., Pugh, T. A. M., Reddy, A., Schmid, E., Jeong, S., Zhou, F., and Piao, S.: Global irrigation contribution to wheat and maize yield, *Nat Commun*, 12, 1235, [https://doi.org/10.1038/s41467-](https://doi.org/10.1038/s41467-021-21498-5)
- 640 021-21498-5, 2021.
- Zhuo, L., Mekonnen, M. M., Hoekstra, A. Y., and Wada, Y.: Inter- and intra-annual variation of water footprint of crops and blue water scarcity in the Yellow River basin (1961–2009), *Advances in Water Resources*, 87, 29–41, <https://doi.org/10.1016/j.advwatres.2015.11.002>, 2016.